

Production of double strange hypernuclei and exotic nuclei in central Au+Au collisions at $\sqrt{s_{NN}}=3$ GeV

N. Buyukcizmeci¹ T. Reichert^{2,3,4}, A.S. Botvina^{2,3}, M. Bleicher^{2,3,5}

¹Department of Physics, Selçuk University, 42079 Campus, Konya, Türkiye

²Institut für Theoretische Physik, J.W. Goethe University, D-60438 Frankfurt am Main, Germany

³ Helmholtz Research Academy Hesse for FAIR (HFHF), GSI Helmholtz Center, Campus Frankfurt, Max-von-Laue-Str. 12, 60438 Frankfurt am Main, Germany

⁴ Frankfurt Institute for Advanced Studies (FIAS), Ruth-Moufang-Str.1, D-60438 Frankfurt am Main, Germany

⁵GSI Helmholtz Center for Heavy Ion Research, Planckstr.1, Darmstadt, Germany

Received: date / Revised version: date

Abstract. We extend the theoretical approach which includes the dynamical and statistical stages for the description of the nucleosynthesis in central collisions of relativistic ions. Previously, this approach was successfully applied to describe experimental data on both normal nuclei and single strange hypernuclei production in the GSI and RHIC-BES energy range. We predict the multiplicities of double strange hypernuclei up to ${}^4_{\Lambda\Lambda}\text{H}$ and further intermediate mass nuclei up to ${}^8\text{Be}$ for Au+Au central collisions at $\sqrt{s_{NN}}=3$ GeV, recently explored by the STAR experiments. These new nuclei can be identified by the measurement of the correlated particles coming after their decay. Such observations are a crucial test for the nucleosynthesis mechanism.

PACS. 25.75.-q , 24.60.-k , 25.70.Pq , 21.65.+f

1 Introduction

The production of novel nuclei (including heavy and exotic ones) has always been an important and interesting topic in nuclear reactions. Typically, such processes include the interactions of multiple particles. A well known example of such a collective process is the compound nucleus formation and its subsequent decay [1,2,3,4], which takes place at low energies (i.e., essentially lower than the nuclear binding energy). The compound nucleus concept was very successful for the description of a large body of reactions (see, e.g., Refs. [5,6] and references therein). Later on, a new collective process was established by studying the multifragmentation reactions: If a considerable amount of energy is deposited in the nucleus (more than 2–3 MeV per nucleon) such nuclear system can expand up to some freeze-out volume, and there the nuclei can be separated from uniform nuclear matter [5,6,7]. This concept was confirmed with experimental and theoretical studies, and the parameters of the freeze-out volume were evaluated. Such a process takes place at subnuclear densities from 0.1 to $0.3\rho_0$ ($\rho_0 \approx 0.15 \text{ fm}^{-3}$ being the ground state nuclear density). The temperatures of such systems are in the range from 5 to 8 MeV. These nuclear matter parameters correspond to the coexistence region in the nuclear liquid-gas type phase transition [8,9,10,11]. Such matter at subnuclear density is the most suitable place for the formation of nuclei involving collective reactions of many

nucleons: Because, 1) at higher densities the formed nuclear clusters are destroyed by the interactions with other nucleons during the matter's expansion, 2) at lower densities the collective nucleation processes are suppressed by too large distances between the nucleons. This reaction picture is consistent with state-of-the-art dynamical calculations describing the fragment formation also (see, e.g., Ref [12,13,14]).

In the previous statistical description of the multifragmentation usually a single freeze-out source was considered in a single reaction event. For example, the source can be associated with highly excited projectile and target residues in peripheral nucleus-nucleus collisions [5]. In this case the relativistic ion collisions open new possibilities to obtain hypernuclei, including multi-strange and exotic nuclei [15,16,17], which are more difficult to produce in other reactions.

During recent years central collisions of relativistic nuclei have been recognized as an important reaction channel leading to the production of novel (exotic) nuclei. A great variety of light complex nuclei can be formed in central heavy-ion reactions [18]. These studies were extended by involving the production of both normal nuclei and hypernuclei, including exotic nuclear species [19,20,21,22,23,24,25,26]. Especially, the nucleosynthesis of strange nuclei can be studied in these processes in great detail. This opens a complementary route to better understand the

nucleosynthesis in the early Universe. It is commonly accepted that light nuclei are mostly formed on later stages of the reaction from baryons which are primary produced [13, 14, 18, 20, 22, 27, 28, 29, 30]. Although other production mechanisms, like a direct thermal production, have been considered [23].

Recently we have proposed and validated a theoretical approach to explain the collective processes leading to the event-by-event production of a large variety of new nuclei in central nucleus collisions: We used the concept of local equilibrium with the formation of several statistical sources in a single reaction event [31, 32, 33]. The comparison with experimental data was very convincing [31, 32]. In addition, we have shown that the STAR experimental data on nuclei and hypernuclei production can also be described in the same way [33]. In this paper we continue our investigation with the STAR central collisions of Au+Au at $\sqrt{s_{NN}}=3$ GeV. We will demonstrate that besides normal and single strange hyper-nuclei many double strange hypernuclei can also be produced in this case. Also, further exotic and short-lived nuclei are predicted. Their experimental identification in the experiment will provide important information on the properties of hypermatter formed by the baryons produced during the initial dynamical stage.

2 Initialization of baryons for the formation of nuclei in low-density matter

The most practical way to describe these reactions is its subdivision into the two stages of different concept: (1) The dynamical interaction of incident nucleons and hadrons inside the nuclear matter leading to the formation of equilibrated nuclear systems, (2) the statistical fragmentation of such systems into individual nuclear fragments with the de-excitation of the hot fragments since they usually include excited states. Various transport models are currently used for the description of the dynamical stage of this reaction by involving binary hadron-hadron collisions at high energies. They take into account the individual particle interactions including the influence of the surrounding matter, the secondary interactions, and the decay of hadron resonances (e.g. [34, 35]). In this case the final particle distribution in the end of the dynamical part preserves important correlations between hadrons originating from the interactions in each event, which are ignored when we consider the final inclusive particle spectra only. Within these kinetic models it was established that many particles participate in these processes by the intensive rescattering leading to the final particle distributions which may look similar to statistical distributions with phase space domination. For example, in peripheral collisions the produced high energy particles leave the system and the remaining (spectator) nucleons form an excited system, a so called residue. We may expect that this system evolves toward a state which is mostly determined by the statistical properties of the excited nuclear matter. The system then expands by both a thermal pressure

and the initial longitudinal motion to a low density and its multifragmentation leads to the production of various new (hyper-)nuclei (see, e.g., [5, 27, 28, 36]). If the excitation energy of the residues is too low to enter the freeze-out state, then the nuclei formation proceeds via a compound nucleus [5]. In the case when hyperons are captured by the residues, the final hypernuclei are produced as a result of the residue's decay [16, 17, 37, 38, 39].

In central nucleus-nucleus collisions another physical picture can be realized: There are practically no spectator nucleons, and all produced baryons have a considerable kinetic energy. After the dynamical stage of the collision the system rapidly expands. At a time around $\sim 20\text{--}40$ fm/c the baryon composition of this matter is established. During the expansion process some of the baryons may be located in the vicinity of each other with local subnuclear densities around $\sim 0.1\rho_0$ ($\rho_0 \approx 0.15$ fm $^{-3}$ being the ground state nuclear density). This nuclear matter density corresponds to the coexistence region in the nuclear liquid-gas type phase transition, and it is the proper place of the synthesis of new nuclei: The remaining attraction between baryons in the diluted matter can then lead to the formation of complex fragments. In the midrapidity kinematic region we expect a substantial production of hyperons, and subsequent hypernuclei production by hyperon capture. The formation process can be simulated as baryon attraction using potentials within the transport models [13, 14, 29], or within phenomenological coalescence models [21, 30, 39, 40, 41]. As we have demonstrated recently [31, 32], the clusterization processes can be effectively described as the statistical formation of nuclei in the low density matter in local chemical equilibrium. We expect that such nucleation processes will mostly produce the light nuclei.

To describe the dynamical reaction part we use the transport model UrQMD [35, 42], which is adapted for these reactions. UrQMD is quite successful in the description of a large body of experimental data on particle production [43, 44]. The produced particles can be located at various rapidities, however, the main part is concentrated in the midrapidity region. After a time of 20–40 fm/c the strong interactions leading to the new particle formation cease and the system start to decouple. Such kind of a freeze-out is general for the transport approaches [45]. In this time-moment we consider the relative space positions and velocities of the baryons. We select the nuclear clusters according to the coordinates and velocities proximity, as was suggested in Refs. [31, 39], and we call it clusterization of baryons (CB). More details on the current UrQMD calculations for Au+Au collisions at $\sqrt{s_{NN}}=3$ GeV and the following CB procedure is provided in Ref. [33]. Here we refrain from a full reiteration and mention only the most important CB parameter, v_c , which determine the maximum relative velocity of baryons inside the clusters respective to its center of mass velocity. As was established previously [31, 32] v_c is within the range of $0.1c - 0.25c$ (that is consistent with the Fermi motion). This parameter is mainly responsible for the cluster size and its excitation.

The main goal of our paper is to investigate the production of double hypernuclei and other very rare nuclear species, which depends essentially on the phase space occupied by baryons. Therefore, in addition to UrQMD, we introduce another method to simulate the baryon velocity distributions after the initial reaction stage. Since the nuclear system expands after the collision in all directions it is possible to use a simplified phenomenological approach for the first reaction stage, in order to investigate the fragmentation mechanisms in detail. Here we use the phase space generation (PSG) method, in which we simulate an expanded nuclear matter state with stochastically distributed baryons: This is the isotropic generation of all baryons of the excited nuclear system according to a microcanonical momentum phase space distribution, with total momentum and energy conservation, corresponding to the one-particle approximation. It is assumed that all particles are in a large volume (at subnuclear densities) where they can still interact with others to populate the phase space uniformly. Technically, this is done using the Monte-Carlo method applied previously in the microcanonical SMM and Fermi-break-up model [5], and taking into account the relativistic effects according to the relativistic connection between momentum \mathbf{p} , mass m , and kinetic energy of particles E_0 , see Eq. (1). In Eq. (1) the sum is over all particles and we use units with $\hbar = c = 1$.

$$\sum \sqrt{\mathbf{p}^2 + m^2} = E_0 + \sum m. \quad (1)$$

The total kinetic energy available for the motion of baryons E_0 (the source energy) is the main parameter which can be adjusted to describe the energy accumulated in the system after the dynamical stage. We have checked that the PSG generated phase space distributions provide a reasonable assumption for the initial stage of the clusterization. Note, that this generation leads to the equilibrium over one-particle degrees of freedom, and it is not an equilibrium with respect to the nucleation process, i.e., it is not a global chemical equilibrium for all baryons in the system. In the PSG case we assume that the coordinates of the baryons are proportional to their velocities and strictly correlate with them as taking place in many explosive processes with strong radial flow.

The main challenge in using the PSG is the correct estimate of the baryon content and the kinetic energy of the baryons in the system. At low (non-relativistic) beam energies, it would be equal to the total number of nucleons times the center of mass energy of the colliding nuclei, in central collisions. However, at relativistic energies many new hadrons are produced and the corresponding energy part should be subtracted, since this part is not participating in the nucleation process. To estimate this energy fraction we use the results obtained by the UrQMD calculations. Then in central Au+Au collisions at $\sqrt{s_{NN}}=3$ GeV we have in average 3.2 produced Λ hyperons per event, and the average center-of-mass kinetic energy is 366 MeV per baryon. For this reason we take the $E_0=366A_0$ MeV for the PSG calculations, with $A_0=394$ including 3 Λ s, here A_0 denotes the total number of baryons considered.

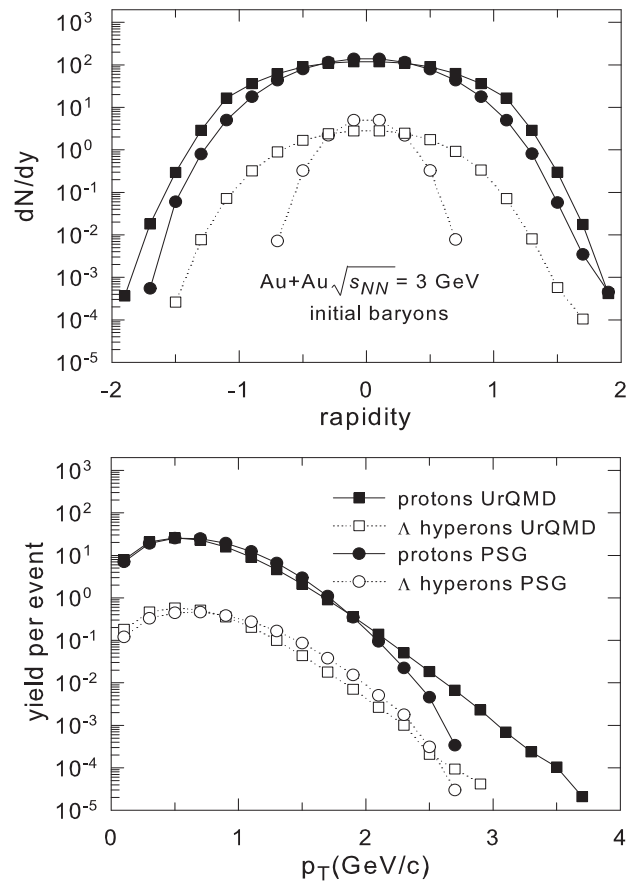


Fig. 1. Total proton and Λ distributions (per event) after UrQMD and PSG calculations of central gold collisions at center-of-mass energy of $\sqrt{s_{NN}}=3$ GeV. Top panel (a) - rapidity distributions. Bottom panel (b) - transverse momenta distributions in the rapidity range $|y| < 0.5$.

In Fig. 1 we show the distributions of protons and Lambda hyperons after the UrQMD simulations in central Au + Au collisions (impact parameters $b \leq 3$ fm) at $\sqrt{s_{NN}}=3$ GeV center-of-mass energy. We show all nucleons and produced hyperons at the cut-off time $t = 20$ fm/c, i.e., after the first hadron interaction inside the nuclei. We have checked that using later times changes our final results only slightly because the interaction rate is rapidly decreasing (see also discussion in Ref. [33]). However, since the baryon coordinates may also be important for the cluster selection after UrQMD, in Figs. 2 and 4 we'll present the comparison of 20 fm/c and 40 fm/c cut-off times.

Also in Fig. 1 the corresponding PSG calculations are presented. Both UrQMD and PSG produce rather broad rapidity and transverse momentum distributions. However, the particle rapidities after PSG are more concentrated around midrapidity (especially for hyperons, since their masses are larger) than in the UrQMD simulations. This difference is due to the dynamical transparency, present in UrQMD since some fast nucleons after rescattering can go through the nuclear matter and interact later with the

secondary hadrons to produce hyperons. This effect does not exist in the phase space simulation with PSG. Such a difference in baryon distributions gives us an opportunity to evaluate the effect of the uncertainty of the initial baryon production on the final production of nuclei.

3 Excited clusters at subnuclear density

In both scenarios (UrQMD and PSG) we subdivide the diluted nuclear matter into multiple clusters with the CB procedure [39,31,32]. Since baryons move relative to each other inside the clusters these clusters present pieces of excited nuclear matter. The selected clusters have a baryon density around $\rho_c \approx \frac{1}{6}\rho_0$: It was established in the previous studies of the statistical multifragmentation process [5,11,46,47,48,49,50,51] that such a density is typical, as a consequence of the liquid-gas type phase transition, for the fragmentation of matter at a low density freeze-out. The excitation energy of such clusters is calculated according to the method given in Refs. [31,32]. In the PSG case we have additionally taken into account the source energy (E_0) and momentum conservation in the system by adjusting these excitation energies. The following evolution of the clusters, including the formation of nuclei from the baryons, is now described in a statistical way. In our model this is described as the decay of hot clusters into light nuclei. For the description of this process we employ the Statistical Multifragmentation Model (SMM) which describes the production of normal nuclei very well, and use its generalization to the hypernuclear case (see Refs. [5,27,28,36,37]).

The results of the selection of the baryonic clusters within CB are shown in Fig. 2 after UrQMD and PSG. We see that the cluster yields decrease nearly power-law like with their masses, and it is similar to a normal coalescence-like process. However, contrary to the coalescence, in our approach these clusters are excited nuclear systems in local chemical equilibrium. The important characteristic is the excitation energy of these clusters, which are presented in the bottom panel. Here we have used the previously established velocity parameter $v_c=0.22c$. As discussed in Ref. [33], the heavier clusters can be formed with larger v_c 's. However, a large v_c leads also to a high excitation energy, since the relative velocity spread of the baryons inside the cluster is higher. A slight time dependence of the cluster sizes for UrQMD is expected: It is obvious that the larger coordinate distances at later times between baryons decrease slightly the production of heavy clusters because of the increased spatial separation. One can see that the PSG leads to larger yields of massive clusters, and this is a very important effect related to the phase space population of the initial baryons. In UrQMD, the initial nucleons are separated from each other in the coordinate space in the very beginning, and after hadron-hadron collisions during the dynamical stage this separation is still preserved and influences the hot cluster selection. Therefore, the clusters in UrQMD are usually smaller than in PSG case, where we assume a direct correlation between the velocities and the coordinates of the nucleons. However,

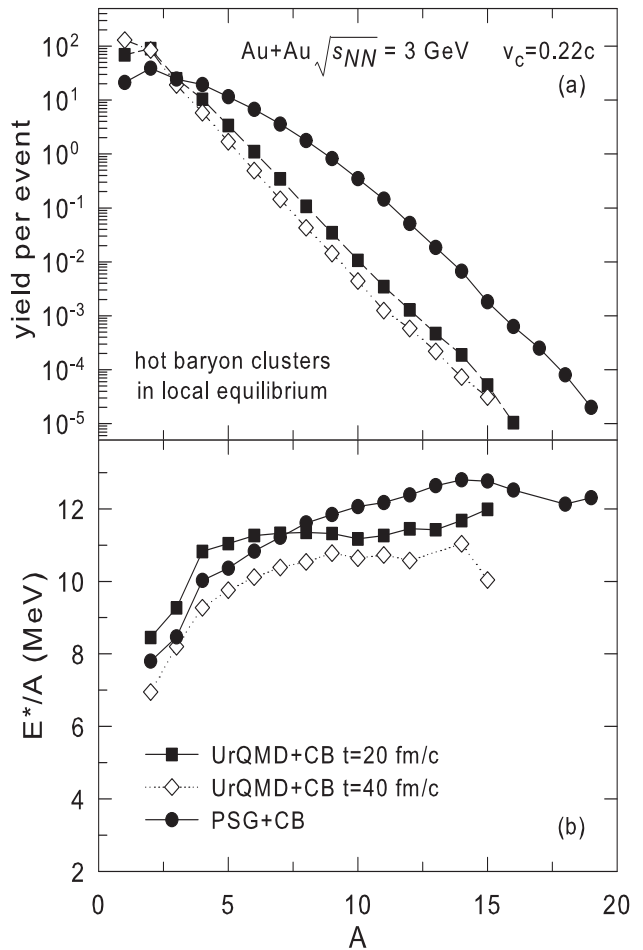


Fig. 2. Comparison of distributions of local nuclear clusters (per event) formed after UrQMD dynamically produced baryons, and PSG statistical simulation for these baryons, by including the CB clusterization procedure which uses the selection of the baryons with the velocity and coordinate proximity. Top panel (a) - mass distributions of the cluster with the velocity parameter $v_c=0.22c$. Bottom panel (b) - average excitation energy of the clusters versus their mass number. The cut-off times for the UrQMD calculations are shown in the panels.

the excitation energies of the clusters remain very similar for all cases and depend mainly on v_c (see [32,33]).

The kinematic characteristics of the primary excited clusters (rapidity and transverse momenta in the center-of-mass system) are depicted in Fig. 3, for $v_c=0.22c$. To evaluate the mass effect we have considered 3 groups of clusters with mass numbers A equal to 2, 4, and 8. One can see that all distributions are quite broad because of the wide momentum distribution of the initial baryons in both UrQMD and PSG cases. The yields of massive clusters are low, that is consistent with Fig. 2. Still there is a difference between UrQMD and PSG: The rapidity distributions of massive clusters (see $A=8$) in the UrQMD case can be partly enhanced by the spectator-like nucleons and be slightly increased towards the projectile and target rapidities.

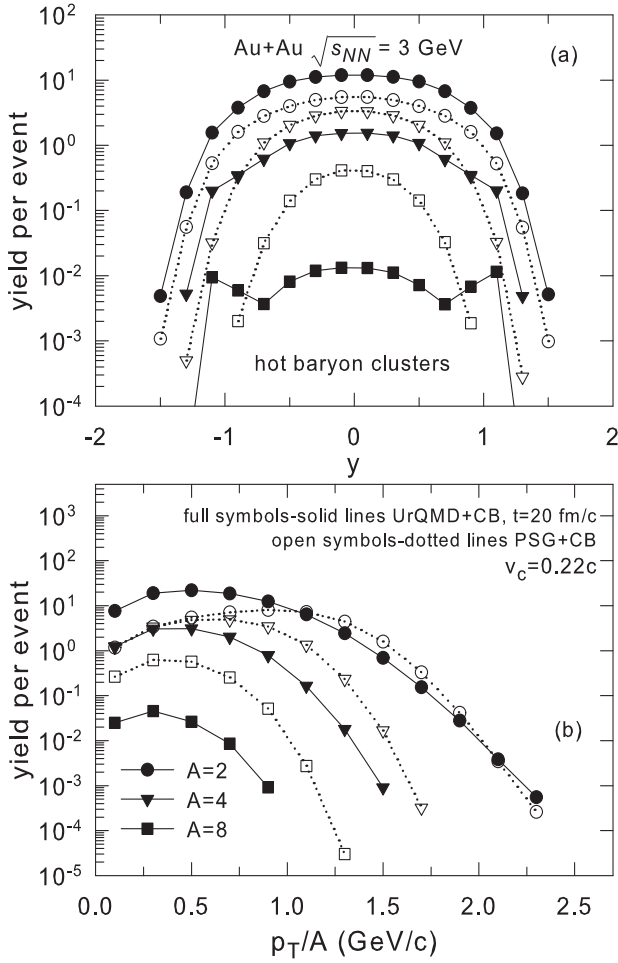


Fig. 3. Yield distributions (per event) of the excited baryon clusters with mass numbers $A=2$, $A=4$, and $A=8$. Top panel (a) - the rapidity (y intervals of 0.2), bottom panel (b) - the transverse momentum per nucleon (p_T/A intervals of 0.2 GeV/c). The calculations are UrQMD+CB (full symbols) and PSG+CB (empty symbols).

4 Production of unstable nuclei and hypernuclei

For further detailed information about the production of new normal nuclei after the decay of such excited clusters we refer to Refs. [31,32]. For example, the products of the cluster decay will preserve the kinematic characteristics (per nucleon) corresponding to the dynamically produced baryons. The isotope production can be explained by assuming the local chemical equilibrium. Many new exotic nuclei can be formed, and the specific correlations of hadrons are the best way to distinguish this reaction mechanism from normal coalescence or direct thermal production. Let us now address a very interesting phenomenon of the formation of short-lived nuclear states and hypernuclei which can be observed in experiments mainly via measuring particle correlations. We make a new suggestion concerning information which can be extracted from the extensive STAR experiment of Au + Au central collisions

at $\sqrt{s_{NN}}=3$ GeV. In Ref. [33] we have demonstrated that the fragment production in these central collisions can be described within our hybrid approach.

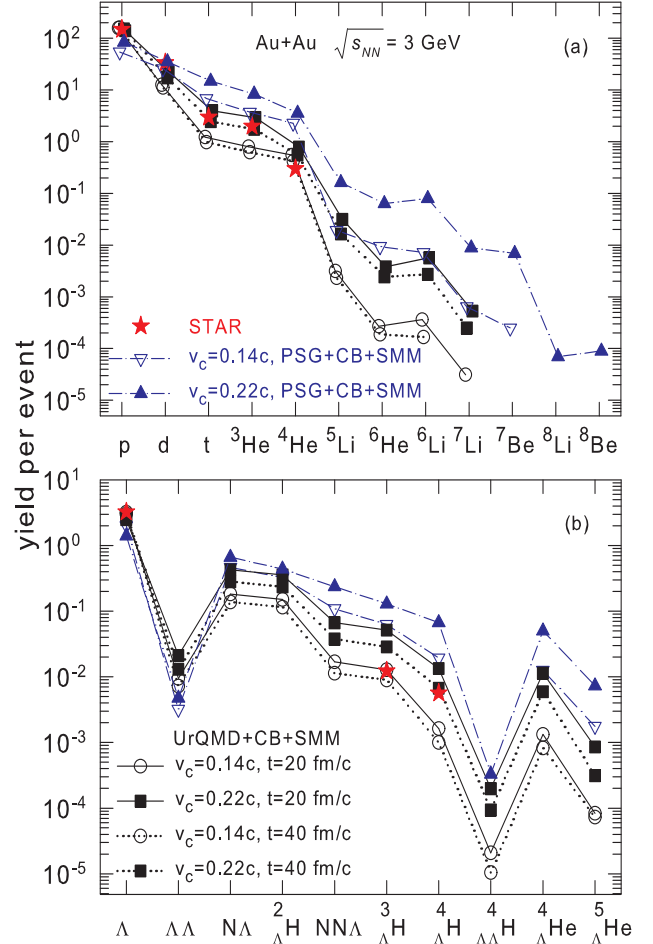


Fig. 4. (Color online.) Comparison of the calculations of final nuclei production including UrQMD (black symbols) and PSG (blue symbols), formation of excited local thermalized clusters (CB) and de-excitation of these clusters (SMM). The STAR experimental data in central collisions (red symbols) are presented too. Top panel (a) - total yields of normal nuclei. Bottom panel (b) - total yields of hypernuclei in central collisions. Notations for nuclei, and the used UrQMD time and v_c parameters are shown in the panels.

In Fig. 4 we show the final state yields of selected light nuclei and hypernuclei (normalized per event) obtained in central collisions. We compare the cold nuclei after the formation and decay chain UrQMD+CB+SMM and PSG+CB+SMM calculations. For convenience we show also the published STAR experimental data [25,52]. As previously established, one generally reaches a good description of the data for normal fragments with the mass numbers range $A = 2-4$ by using for UrQMD the velocity parameter $v_c=0.22c$, which corresponds to the hot cluster excitation energies around 10 MeV per nucleon (see Fig. 2

and the discussion in Ref. [33]). For PSG case this parameter can be lower since the primary baryon clusters are bigger. However, both parameter sets are consistent with the parameter values extracted from the analyses of FOPI experimental data [31,32].

The yields manifest the expected power-law decreasing with A . Nevertheless, we predict a substantial amount of nuclei with $A \geq 4$. Such nuclei are very important for the understanding of the nucleation mechanism. For this reason, first, let us consider normal nuclei (top panel). We predict a relatively large yields of unstable ${}^5\text{Li}$ nuclei (in the excited level of 16.8 MeV), which decays mainly into proton and ${}^4\text{He}$ [53,54] after a time of around 10^3 fm/c. The corresponding correlations can be observed in experiment, since the decay time of this state is substantially longer than its formation time in this multifragmentation reaction, which is less than 100 fm/c. One also observes considerable yields of stable and long-lived Li and Be nuclei. The measurement of such massive nuclei in high energy reaction in the midrapidity zone would an important confirmation of the local chemical equilibrium process. It is very difficult to explain the production of nuclei with $A > 4$ within a simplistic coalescence model or within a global equilibrium hypothesis (with very high temperature). We suggest to measure correlations of particles coming from decays of unstable massive nuclei. For example, ${}^8\text{Be}$ nuclei can decay into two ${}^4\text{He}$ nuclei after a prolonged time of 10^{-16} sec. We predict a substantial yield of ${}^8\text{Be}$ (around $10^{-4} - 10^{-5}$ per central event) by using PSG nucleon distributions. The experimental observation of such a correlation would indicate that nuclei with $A=6-7$ should be produced too. Within the present version of UrQMD we have estimated that the probability to produce these nuclei is very small ($\lesssim 10^{-6}$). Because with the baryon distributions from UrQMD one obtains few large primary hot clusters. However, this probability may be higher within other considerations of the dynamical stage by using other model parameters or other dynamical models [31]. For all initial baryon distributions one can use the same statistical prescription describing the nuclei formation from neighbour baryons. A natural way for the identification of the reaction mechanism is the experimental observation of the particle correlation after decays of primary hot clusters, unstable nuclei and hypernuclei [31]. We emphasize especially that for such many-body phenomena the correlations provide the most effective method to unveil the real formation process among many alternatives.

In relativistic collisions the yields of hypernuclei are very abundant, and we demonstrate it in the bottom panel of Fig. 4. It is instructive to extend the nuclear chart into the strangeness sector, because hypernuclei can provide information on the hyperon interaction in nuclear matter, and on the properties of hypermatter, that is also important in astrophysical environment (see, e.g., Refs. [55,56,57,58,59,60,61]). In addition, the suggested fragment formation mechanism realized in heavy ion collisions allows for investigating hypermatter at subnuclear densities. The production of hypernuclei as a result of decay of excited

nuclear hyper-clusters was first addressed in peripheral ion collisions and hadron reactions [62]. In the reaction under consideration, see Ref. [33], we have discussed the production of well known light single strange hypernuclei. Here we present also the predictions for exotic/unknown single strange hypernuclei, in particular, $\Lambda\Lambda$, ${}^2_\Lambda\text{H}$, and $\text{NN}\Lambda$ hypernuclei. It is interesting that the ground state hypernuclei with $A=2$ were not observed in the traditional hyper-nuclear experiments by using hadron/lepton beams. To this aim relativistic ion collisions provide new opportunities. In our theoretical approach we are able to consider both deeply-bound and short-lived excited states of these nuclei, if they exist. For a first rough estimate we have assumed that such nuclei have a very low hyperon binding energy of 0.05 MeV. It is encouraging that $\text{NN}\Lambda$ hypernucleus was reported in Ref. [63]. Therefore, it would be interesting to verify their existence in new experiments with relativistic ions.

In this work we have increased the statistics of the UrQMD calculations for central collisions up to 96000 events, and we point at the possibility to produce double hypernuclei. One of the open puzzles of the hypernuclear physics is still the H-dibaryons, i.e., the bound $\Lambda\Lambda$ systems, which have been discussed for many years (see, e.g., Refs. [62,64,65,66]). In the present calculations we have assumed a zero binding for the ground state and still obtain a quite large amount of $\Lambda\Lambda$, around 10^{-2} per event. Strange H-dibaryons were not observed in experiments up to now. The reason may be that their lifetime is too short. Nevertheless, they may be seen in the correlation measurement by decay products in modern experiments. If we assume that there exists a deeply-bound state or relatively long-lived excited state then its yield may be several times higher or lower. However, it will be sufficiently high to be measured by particle correlations according to our predictions. It is further very instructive to measure ${}^4_{\Lambda\Lambda}\text{H}$ hypernuclei in the well known ground-state. We predict these nuclei at the level of $10^{-5} - 10^{-4}$ for all calculation scenarios. A possible many-particle correlation to detect these hypernuclei might be ${}^4_{\Lambda\Lambda}\text{H} \rightarrow \pi^- + {}^4_\Lambda\text{He}$, and then ${}^4_\Lambda\text{He} \rightarrow \pi^- + p + {}^3\text{He}$. There was suggested recently that the double strange hypernuclei consisting of two Λ s and two neutrons (i.e., ${}^4_{\Lambda\Lambda}\text{n}$) may exist [67]. We have estimated from our calculation that, by assuming their binding energy in a low limit of 0.05 MeV, their yield would be several times smaller than the yield of ${}^4_{\Lambda\Lambda}\text{H}$. The observation of double strange hypernuclei and the comparison with the yields of single strange hypernuclei and normal nuclei will allow to investigate hyper-matter and hyperon-hyperon interaction at subnuclear density. This is a direct consequences of the statistical regularities of the production mechanism at the nucleation stage [38].

5 Conclusions

We have applied a new theoretical approach to explain the yields of conventional light nuclei (including exotic/unstable ones) and single/double strange hypernuclei which can be

measured in relativistic ion experiments in central nucleus-nucleus collisions. Our approach combines 1) the adequate dynamical and statistical models to find the distributions of baryons produced in the first reaction stage, 2) the formation of intermediate local sources in chemical equilibrium (excited multi-baryonic clusters) at subnuclear density, and 3) the description of the nucleation process inside these sources as their statistical decay. A special theoretical development of this work is the suggestion to use PSG method for the initial baryon distributions with general characteristics of nuclear matter taken from UrQMD calculations. This provides a chance to evaluate the effect of the variation of the initial baryon distributions on the nucleosynthesis. As was shown previously [31,32] our approach can be successfully used to analyze the production of non-strange nuclei. We have demonstrated that the STAR experimental data concerning the production of nuclei and hypernuclei at a high collision energy can also be described within this approach by using similar parameters for the local sources. This may indicate a universal character of the nucleation process in rapidly expanding nuclear matter. We point out that the large variety and abundance of produced hypernuclei is an important advantage of relativistic heavy ion collisions in comparison with the traditional hypernuclear methods concentrated on reactions leading only to a few species.

Previously nucleosynthesis was under examination mostly for stable nuclei. Now we reach the next stage where also unstable conventional nuclei (e.g., ${}^5\text{Li}$, ${}^8\text{Be}$), single and double hypernuclei can be produced in the same reaction events. We suggest that some problems of the hypernuclear physics can be resolved by involving these reactions in which there is a great yield of exotic nuclei, e.g., H-dibaryons. In addition, we predict a considerable production of ${}^4_{\Lambda\Lambda}\text{H}$ hypernuclei, which were already observed in other hypernuclear experiments. The production rate of these nuclei is high enough for their detection. By comparing the yields of different hypernuclei one can extract important information about hypermatter in which the nuclei are formed, and about the properties of exotic hypernuclei [33,38]. This information is also of utmost importance in astrophysics for models describing stellar matter in supernova explosions and in binary neutron star mergers. Big hypernuclear isotopes and double hypernuclei can be singled out from large pieces of hypernuclear matter in local chemical equilibrium. Therefore, their formation process can provide complementary information on the matter, and a deeper knowledge on the hyper-nucleosynthesis at low densities will be obtained. The correlation measurements in the experiments and the comparison of different nuclei/hypernuclei yields in same reactions are a straightforward method to obtain this new information.

The authors acknowledges German Academic Exchange Service (DAAD) support from a PPP exchange grant and the Scientific and Technological Research Council of Türkiye (TUBITAK) support under Project No. 121N420. T.R. acknowledges support through the Main-Campus-Doctus fellowship provided by the Stiftung Polytechnische Gesellschaft Frankfurt am Main and further thanks the Samson AG for

their support. N.B. thanks J.W. Goethe University Frankfurt am Main for hospitality. Computational resources were provided by the Center for Scientific Computing (CSC) of the Goethe University and the "Green Cube" at GSI, Darmstadt.

References

1. N. Bohr, Nature **137**, 344 (1936).
2. N. Bohr and J. Wheeler, Phys. Rev. **56**, 426 (1939).
3. V. Weisskopf, Phys. Rev. **52**, 295 (1937).
4. T. Ericson, Adv. in Phys. **9**, 425 (1960).
5. J. P. Bondorf, A. S. Botvina, A. S. Iljinov, I. N. Mishustin and K. Sneppen, Phys. Rep. **257**, 133 (1995).
6. A.S. Botvina and I.N. Mishustin, Eur. Phys. J. **A 30**, 121 (2006).
7. D.H.E. Gross, Rep. Progr. Phys. **53**, 605 (1990).
8. G. Sauer, H. Chandra and U. Mosel, Nucl. Phys. A **264**, 221 (1976).
9. H.R. Jaqaman, A.Z. Mekjian and L. Zamick, Phys. Rev. C **31**, 2067 (1984).
10. A.D. Panagiotou, M.W. Curtin and D.K. Scott, Phys. Rev. C **29**, 55 (1985).
11. V. A. Karnaukhov *et al.*, Phys. At. Nucl. **69**, 1142 (2006).
12. A. Ono, JPS Conf. Proc. **32**, 010076 (2020).
13. A. Le Fevre, J. Aichelin, C. Hartnack, Y. Leifels, Phys. Rev. C **100**, 034904 (2019).
14. J. Aichelin, E. Bratkovskaya *et al.*, Phys. Rev. C **101**, 044905 (2020).
15. A.S. Botvina, M. Bleicher, J. Pochodzalla and J. Steinheimer, Eur. Phys. J. A **52**, 242 (2016).
16. A. S. Botvina *et al.*, Phys. Rev. C **95**, 014902 (2017).
17. A. S. Botvina *et al.*, Phys. Rev. C **88**, 054605 (2013).
18. J. Gosset, H. H. Gutbrod, W. G. Meyer, A. M. Poskanzer, A. Sandoval, R. Stock, and G. D. Westfall, Phys. Rev. C **16**, 629 (1977).
19. W. Reisdorf *et al.*, Nucl. Phys. A **612**, 493 (1997).
20. W. Neubert and A. S. Botvina, Eur. Phys. J. A **17**, 559 (2003).
21. W. Neubert and A. S. Botvina, Eur. Phys. J. A **7**, 101 (2000).
22. W. Reisdorf *et al.*, Nucl. Phys. A **848**, 366 (2010).
23. A. Andronic, P. Braun-Munzinger, J. Stachel, H. Stöcker, Phys. Lett. B **697**, 203 (2011).
24. J. Adam *et al.*, ALICE Collaboration, Phys. Lett. B **754**, 360 (2016).
25. M. S. Abdallah *et al.*, STAR Collaboration, Phys. Rev. Lett. **128**, 202301 (2022).
26. R. Abou Yassine *et al.*, HADES Collaboration, EPJ Web of Conferences **271**, 08004 (2022).
27. R. Ogul *et al.*, Phys. Rev. C **83**, 024608 (2011).
28. R. P. Scharenberg, B. K. Srivastava, S. Albergo, F. Bieser, F. P. Brady, Z. Caccia *et al.*, Phys. Rev. C **64**, 054602 (2001).
29. S. Glässel *et al.*, Phys. Rev. C **105**, 014908 (2022).
30. V. D. Toneev, K. K. Gudima, Nucl. Phys. A **400**, 173 (1983).
31. A. S. Botvina, N. Buyukcizmeci and M. Bleicher, Phys. Rev. C **103**, 064602 (2021).
32. A. S. Botvina, N. Buyukcizmeci and M. Bleicher, Phys. Rev. C **106**, 014607 (2022).
33. N. Buyukcizmeci, T. Reichert, A.S. Botvina, and M. Bleicher, Phys. Rev. C **108**, 054904 (2023).

34. J. Aichelin, Phys. Rep. **202**, 233 (1991).
35. M. Bleicher *et al.*, J. Phys. G **25**, 1859 (1999).
36. A. S. Botvina and J. Pochodzalla, Phys. Rev. C **76**, 024909 (2007).
37. A. S. Lorente, A. S. Botvina, and J. Pochodzalla, Phys. Lett. B **697**, 222 (2011).
38. N. Buyukcizmeci *et al.*, Phys. Rev. C **98**, 064603 (2018).
39. A. S. Botvina *et al.*, Phys. Lett. B **742**, 7 (2015).
40. A. S. Botvina, J. Steinheimer, M. Bleicher, Phys. Rev. C **96**, 014913 (2017).
41. S. Sombun, K. Tomuang, A. Limphirat, P. Hillmann, C. Herold, J. Steinheimer, Y. Yan, M. Bleicher, Phys. Rev. C **99**, 014901 (2019).
42. S.A. Bass *et al.*, Prog. Part. Nucl. Phys. **41**, 255 (1998).
43. T. Reichert *et al.*, J. Phys. G **49**, 055108 (2022).
44. T. Reichert *et al.*, Phys. Rev. C **107**, 014912 (2023).
45. A. S. Botvina, K. K. Gudima, J. Steinheimer, M. Bleicher, I. N. Mishustin, Phys. Rev. C **84**, 064904 (2011).
46. B.-A. Li, A. R. DeAngelis and D. H. E. Gross, Phys. Lett. B **303**, 225 (1993).
47. H. Xi *et al.*, Z. Phys. A **359**, 397 (1997).
48. M. D'Agostino *et al.*, Phys. Lett. B **371**, 175 (1996).
49. N. Bellaize *et al.*, Nucl. Phys. A **709**, 367 (2002).
50. J. Iglio *et al.*, Phys. Rev. C **74**, 024605 (2006).
51. V. E. Viola *et al.*, Nucl. Phys. A **681**, 267c (2001).
52. Hui Liu for STAR Collaboration, Acta Phys. Polon. B, Proc. Suppl. **16**, 1–A148 (2023).
53. F. Ajzenberg and T. Lauritsen, Rev. Mod. Phys. **27**, 77 (1955).
54. F. Ajzenberg-Selove and T. Lauritsen, Nucl. Phys. **11**, 1 (1959).
55. M. Wakai, H. Bando, M. Sano, Phys. Rev. C **38**, 748 (1988).
56. H. Bando, T. Mottle, and J. Zofka, Int. J. Mod. Phys. **A5**, 4021 (1990).
57. J. Schaffner *et al.*, Phys. Rev. Lett. **71**, 1328 (1993).
58. J. Schaffner and I.N. Mishustin, Phys. Rev. C **53**, 1416 (1996).
59. O. Hashimoto, H. Tamura, Prog. Part. Nucl. Phys. **57**, 564 (2006).
60. A. Gal, E.V. Hungerford, and D.J. Millener, Rev. Mod. Phys. **88**, 035004 (2016).
61. E. Hiyama and K. Nakazawa, Annu. Rev. Nucl. Part. Sci., **68**, 131 (2018).
62. A. S. Botvina, I.N. Mishustin, and J. Pochodzalla, Phys. Rev. C **86**, 011601(R) (2012).
63. C. Rappold *et al.* (HypHI Collaboration), Phys. Rev. C **88**, 041001(R) (2013).
64. R.L. Jaffe, Phys. Rev. Lett. **38**, 195 (1977).
65. J. Steinheimer *et al.*, Phys. Lett. B **714**, 85 (2012).
66. A. Gal, arXiv:2404.12801 (2024).
67. S. Bleser *et al.*, Phys. Lett. B **790**, 502 (2019).